Published in final edited form as:
Exp Neurol. 2011 July ; 230(1): 96–105. doi:10.1016/j.expneurol.2011.04.001.

Amygdalar peptidergic circuits regulating noradrenergic locus coeruleus neurons: linking limbic and arousal centers

B. A. S. Reyes, **A. F. Carvalho**, **K. Vakharia**, and **E. J. Van Bockstaele**
Department of Neuroscience, Farber Institute for Neurosciences, Thomas Jefferson University, Philadelphia, PA 19107

Abstract

The endogenous opioid peptides, met- or leu-enkephalin, and corticotropin-releasing factor (CRF) regulate noradrenergic neurons in the locus coeruleus (LC) in a convergent manner via projections from distinct brain areas. In contrast, the opioid peptide dynorphin (DYN) has been shown to serve as a co-transmitter with CRF in afferents to the LC. To further define anatomical substrates targeting noradrenergic neurons by DYN afferents originating from limbic sources, anterograde tract-tracing of biotinylated dextran amine (BDA) from the central amygdaloid complex was combined with immunocytochemical detection of DYN and tyrosine hydroxylase (TH) in the same section of tissue. Triple labeling immunocytochemistry was combined with electron microscopy in the LC where BDA was identified using an immunoperoxidase marker, and DYN and TH were distinguished by the use of sequential immunogold labeling and silver enhancement to produce different sized gold particles. Results show direct evidence of a monosynaptic pathway linking amygdalar DYN afferents with LC neurons. To determine whether DYN-containing amygdalar LC projecting neurons colocalize CRF, retrograde tract-tracing using fluorescent latex microspheres injected into the LC was combined with immunocytochemical detection of DYN and CRF in single sections in the central amygdala. Retrogradely labeled neurons from the LC were distributed throughout the rostro-caudal extent of the central nucleus of the amygdala (CeA) as previously described. Cell counts showed that approximately 42% of LC-projecting neurons in the CeA contained both DYN and CRF. Taken with our previous studies showing monosynaptic projections from amygdalar CRF neurons to noradrenergic LC cells, the present study extends this by showing that DYN and CRF are co-transmitters in monosynaptic projections to the LC and are poised to coordinately impact LC neuronal activity.

Keywords

DYN; tyrosine hydroxylase; BDA; locus coeruleus; electron microscopy

Introduction

The dynorphin (DYN)-kappa opioid receptor (κOR) system has been implicated as an important mediator of stress and drug abuse vulnerability. We have shown that DYN is

Corresponding Author: Beverly A. S. Reyes, D.V.M., Ph.D., Department of Neuroscience, Farber Institute for Neurosciences, Thomas Jefferson University, 900 Walnut Street, Suite 400, Philadelphia, PA 19107, Voice: (215) 503-5857, FAX: (215) 503-9238, bsr103@jefferson.edu.

localized in axon terminals in the locus coeruelus (LC) (Reyes et al., 2007b, Reyes et al., 2008, Reyes et al., 2009), the major norepinephrine containing nucleus that innervates almost all levels of the neuraxis (Foote et al., 1983, Aston-Jones et al., 1984, Aston-Jones et al., 1991). While it is known that interactions of stress and opioid substrates occur in various brain regions that may play a role in drug dependence and withdrawal (McNally and Akil, 2002, Houshyar et al., 2003, Maj et al., 2003), the LC is one site at which opioids and stress substrates may interact to have global effects on behavior.

The LC receives afferents from multiple brain regions including the central nucleus of the amygdala (CeA) (Van Bockstaele et al., 1996a, Van Bockstaele et al., 1998, Van Bockstaele et al., 1999b). Anterograde tract-tracing studies using biotinylated dextran amine (BDA) injected into the CeA showed that BDA-labeled axon terminals target tyrosine hydroxylase (TH)-containing LC neurons (Van Bockstaele et al., 1996a, Van Bockstaele et al., 1999b). Further studies following electrolytic lesions of the CeA demonstrated decreases in corticotropin-releasing factor (CRF) immunoreactivity in the LC, on the side ipsilateral to the lesion (Tjoumakaris et al., 2003, Reyes et al., 2008). Likewise, electrolytic lesions of the CeA significantly reduced DYN immunoreactivity in the LC (Reyes et al., 2008). Though anatomical, lesioning and tract-tracing studies have supported CeA innervation of the LC by DYN afferents (Reyes et al., 2007b, Reyes et al., 2008), whether DYN-containing neurons from the CeA form monosynaptic projections with TH-labeled dendrites in the LC has not been definitively established. Thus, in the first part of the present study, anterograde tract-tracing of BDA from the CeA was combined with immunocytochemical detection of DYN and TH in the LC to unequivocally establish that amygdalar afferents form synaptic contacts with noradrenergic neurons in the LC. Triple labeling immunohistochemistry was combined with electron microscopy in the LC where BDA was identified using an immunoperoxidase marker, and DYN and TH were distinguished using different sized immunogold-silver particles.

Electrophysiological studies have demonstrated that activity of the LC-norepinephrine system is co-regulated by CRF and endogenous opioids, such that the onset of stress releases CRF within the LC to activate this system with the consequence of increased arousal and a shift from focused to scanning attention (Valentino et al., 1991, Curtis et al., 2001). The termination of stress engages endogenous opioid peptide release that inhibits the system and returns LC neuronal activity back to baseline (Valentino et al., 1991, Curtis et al., 2001). The finding that CRF and opioids regulate the activity of the LC-norepinephrine system during stress in an opposing manner is further supported by anatomical data showing prominent co-existence of CRF receptors and mu-opioid receptors in LC neurons (Reyes et al., 2007a). We have reported co-existence of CRF and DYN in the CeA (Reyes et al., 2008). Moreover, lesions of the CeA (described above) showed a significant reduction of CRF and DYN immunoreactivities in the LC (Tjoumakaris et al., 2003, Reyes et al., 2008). Although convergent lines of evidence support co-regulation of LC neurons by CRF and DYN, the source of afferents containing DYN and CRF to the LC has not been determined. Therefore in a second study, we determined the neurochemical phenotype of amygdalar projections to the LC that co-express DYN and CRF by using retrograde tract-tracing of fluorescent latex microspheres from the LC combined with immunocytochemical labeling of DYN and CRF with fluorescent-tagged secondary antibodies in the CeA.

Materials and Methods

All procedures used in the present study were approved by the Institutional Animal Care and Use Committee of Thomas Jefferson University and conformed with *National Institutes of Health Guide for the Care and Use of Laboratory Animals* guidelines. Rats were housed 2–3 per cage on a 12-h light schedule (lights on at 0700) in a temperature-controlled (20 ºC)

colony room. They were allowed ad libitum access to standard rat chow and water. Rats were allowed to acclimate to the animal housing facility for several days prior to the onset of the study. All efforts were made to utilize only the minimum number of animals necessary to produce reliable scientific data and attempts were made to minimize any animal distress.

Experimental Animals

Adult male Sprague-Dawley rats (Harlan Sprague-Dawley, Inc., Indianapolis, IN) weighing 250–300 g were used in this study. Eight rats were injected with fluorescent latex microspheres (Lumafluor Corp., Naples, FL) into the LC. Sixteen rats were injected with biotinylated dextran amine (BDA) into the CeA. Specificity of antibodies and control sections

The rat preprodynorphin (ppDYN) antiserum raised against residues 235–248 (SQENPNTYSEDLDV) was generated in guinea pig (Arvidsson et al., 1995). The specificity of ppDYN antiserum was tested by absorption controls with the cognate peptides (Arvidsson et al., 1995, Reyes et al., 2007b). Preabsorption of ppDYN with the antigenic peptide at 0.1 to 1 μM blocked DYN immunoreactivity (Arvidsson et al., 1995). There was no detectable immunoreactivity observed when tissue sections were processed in the absence of the primary antibody (Reyes et al., 2007).

The CRF serum (lot C70) was raised in rabbit and was generated against the human/rat CRF peptide (SEEPPISLDLTFHLLREVLEMARAEQLAQQAHSNRKLMEIINH2), conjugated to human α-globulins. The antibody has been found in radioimmunoassay to recognize the NH2 terminus (residues 4–20) of ovine hypothalamic CRF (Rivier et al., 1983a). The specificity of the CRF serum was tested by incubating sections in primary CRF antiserum preabsorbed for 24 hours with CRF at 1 mg/ml. Specific immunoreactivity was eliminated by prior absorption with its immunogen at 1 mg/ml and 10 mg/ml (Sawchenko et al., 1984, Van Bockstaele et al., 1996b). An immunodot blot showed that the CRF antiserum used in the present study exhibited intense recognition of the parent antigen CRF and no cross-reactivity with any of the dilutions of other peptides including melanin-concentrating hormone or α-melanocyte-stimulating hormone (Van Bockstaele et al., 1996b).

The immunogen for mouse monoclonal antiserum was raised against denatured TH from rat pheochromocytoma, labels a single band at approximately 62kD corresponding to TH, and does not cross-react with dopamine-β-hydroxylase, dihydropterdine reductase, phenylethanolamine-N-methyltransferase, phenylalanine hydroxylase or tryptophan hydroxylase. The antibody has a wide species cross-reactivity. The specificity of the TH antibody has been examined by preabsorption of the antibody with a high concentration of TH (Van Bockstaele and Pickel, 1993).

All control experiments were carried out where tissue sections were processed in the absence of primary antibodies. These tissue sections were processed in parallel with tissue sections incubated with primary antibodies. In control tissue sections, no DYN, CRF or TH immunoreactivity was detected using either immunofluorescence or electron microscopy.

Anterograde and retrograde transport: surgery

Animals injected with BDA into the CeA were initially anesthetized with a cocktail of ketamine hydrochloride (100 mg/kg; Phoenix Pharmaceutical, Inc., St. Joseph, MO) and xylazine (2mg/kg; Phoenix Pharmaceutical, Inc., St. Joseph, MO) in saline intraperitoneally (i.p.) and placed in a stereotaxic apparatus for surgery. Anesthesia was supplemented with isoflurane (Abbott Laboratories, North Chicago, IL; 0.5–1.0%, in air) via a specialized nose cone affixed to the incisor bar of the stereotaxic frame (Stoelting Corp., Wood Dale, IL). Glass micropipettes (Kwik-Fil, 1.2 mm outer diameter; World Precision Instruments, Inc.,

Sarasota, FL) with tip diameters of 15–20 μm were filled with 10% BDA (10,000 molecular weight, Molecular Probes, Eugene, OR, USA) in 0.1 M phosphate buffer (PB; pH 7.4). The tips of glass micropipettes were positioned in the CeA using the following coordinates: 2.3 mm posterior from the bregma and 4.2 mm medial/lateral based on the rat brain atlas of Paxinos and Watson (1986). The glass micropipettes were lowered targeting the appropriate coordinates for placement of BDA into the CeA (6.7 mm ventral from the top of the skull). BDA was injected using a Picospritzer (Genreal Valve Corporation, Fairfield, NJ) at 24–26 psi, 10 ms duration and 0.2 Hz. Injection of BDA was done unilaterally into the CNA of each animal. Pipettes were left at the site of injections for 5 min after tracer deposit to limit leakage of the tracer along the pipette track. The survival period determined to be optimal for detection of anterograde labeling in the LC was 7 to 10 days as previously reported in a prior study (Reyes et al., 2005). Rats were deeply anesthetized with sodium pentobarbital (60 mg/kg, i.p.; Ovation Pharmaceuticals, Inc., Deerfield, IL) and perfused through the ascending aorta with (1) 10 ml heparin, (2) 50 ml of 3.75% acrolein (Electron Microscopy Sciences, Fort Washington, PA), and (3) 2% formaldehyde in 0.1 M PB. Twenty hours prior to transcardial perfusion, rats received injections of colchicine (50 μg; Sigma Immunochemical) into each lateral ventricle. Immediately following perfusion, brains were removed and sliced into 2–3 mm coronal pieces of tissue and were postfixed in 2% formaldehyde overnight at 4°C. Coronal sections in 40 μm thickness were cut on a Vibratome (Technical Product International, St. Louis, MO) and collected into 0.1 M PB.

For retrograde tract-tracing, burr holes were drilled on the skull using coordinates obtained from the rat brain atlas of Paxinos and Watson (1986): for the LC, coordinates were 10.04 mm posterior from the bregma, 1.4 mm medial/lateral and 7.1 mm ventral from the top of the skull. Glass micropipettes with tip diameters of 15–20 μm were filled with green or red fluorescent latex microspheres. The tips of the glass micropipettes were lowered to the appropriate area for deposit of fluorescent latex microspheres into the LC. Rats were transcardially perfused through the ascending aorta with heparin followed by 4% formaldehyde in 0.1 M PB. Twenty hours prior to transcardial perfusion, rats received injections of colchicine (50 μg; Sigma Immunochemical) into each lateral ventricle. The brains were removed, blocked, immersed in 4% formaldehyde overnight at 4°C, and stored in 30% sucrose solution in 0.1 M PB containing 0.1% sodium azide at 4°C for few days. The side of the brain contralateral to the injection was notched to verify tissue orientation following sectioning.

Anterograde tract-tracing: immunohistochemistry

As previously described, BDA was visualized by an immunohistochemical reaction (Reyes et al., 2005). Briefly, sections through the CeA and LC were rinsed in 0.1 M PB followed by 0.1 M tris-buffered saline (TBS; pH 7.6) and incubated for 2 hours in avidin-biotin complex (ABC Elite Kit, Vector Laboratories, Burlingame, CA) solution at room temperature. After thorough rinsing, the tissue sections were immersed for 10 minutes in a solution containing 22 mg of 3-3′ diaminobenzidine (DAB; Aldrich, Milwaukee, WI) and 10 μl of 30% hydrogen peroxide (H_2O_2) in 100 ml of 0.1 M TBS.

Triple immunolabeling: immunoperoxidase and sequential immunogold-silver labeling

Following visualization of BDA by immunohistochemical reaction, the tissue sections were further processed for dual immunogold-silver labeling for DYN and TH. We followed the procedure for dual immunogold-silver labeling that we recently described in another study (Jin et al., 2010). Tissue sections were incubated for 12–16 hours in a cocktail containing guinea pig anti-prodynorphin (ppDYN; Neuromics, Inc., Minneapolis, MN) at 1:2,000 and mouse anti-TH (Immunostar Inc., Hudson, WI, USA) at 1:1000. Thereafter, sections were rinsed extensively in 0.1 M TBS and 0.2% bovine serum albumin (BSA) in 0.01 M

phosphate-buffered saline (PBS) followed by incubation in goat anti-guinea pig IgG ultra-small conjugate (1:100; Amersham Bioscience Corp., Piscataway, NJ, USA) at room temperature for 2 hours. Tissue sections were rinsed six times in 0.2% BSA-0.01 M PBS and twice in 0.1 M PB. Pre-enhancement washings were done with Enhancement Conditioning Solution (ECS; Amersham Bioscience Corp.) followed with the first silver enhancement (300 μl R-Gent SE-EM enhancement mixture; Amersham Bioscience Corp.) for 90 min. Subsequently, tissue sections were rinsed in 0.2 M citrate buffer, four times in ECS and two times in 0.1 M PB and were incubated in goat anti-mouse IgG ultra-small conjugate (1:100; Amersham Bioscience Corp.) at room temperature for 2 hours followed by rinses with 0.2% BSA-0.01 M PBS and 0.1 M PB. Then, sections were incubated in 2.5% glutaraldehyde (Electron Microscopy Sciences) in 0.01 M PBS for 2 hours followed by extensive rinses with 0.1 M PB and distilled water. The second silver enhancement (300 μl R-Gent SE-EM enhancement mixture; Amersham Bioscience Corp.) was performed for 60 min. Tissues sections were washed extensively with distilled water and 0.1 M PB. All washes were done at 10 min-intervals. Following washes, tissue sections were incubated in 2% osmium tetroxide (Electron Microscopy Sciences) in 0.1 M PB for 1 h, washed in 0.1 M PB, dehydrated in an ascending series of ethanol followed by propylene oxide and flat embedded in Epon 812. Thin sections of approximately 50–80 nm in thickness were cut with a diamond knife (Diatome-US, Fort Washington, PA, USA) using a Leica Ultracut (Leica Microsystems, Wetzlar, Germany). Sections were collected on copper mesh grids, examined with an electron microscope (Morgagni, Fei Company, Hillsboro, OR, USA) and digital images were captured using the AMT advantage HR/HR-B CCD camera system (Advance Microscopy Techniques Corp., Danvers, MA, USA). Figures were assembled and adjusted for brightness and contrast in Adobe Photoshop CS4 software (Adobe Systems, Inc., San Jose, CA).

Retrograde tract-tracing: immunohistochemistry

Rat brains were frozen using Tissue Freezing Medium (Triangle Biomedical Science, Durham, NC). Frozen 30 μm-thick sections were cut through the LC and CeA using a freezing microtome (Micron HM550 cryostat; Richard-Allan Scientific, Kalamazoo, MI) and rinsed extensively in 0.1 M PB and 0.1 M TBS. Subsequently, every fourth section through the LC and the CeA was mounted on gelatinized coated slides, allowed to dry and coverslipped using Krystalon mounting medium (EM Industries, Gibbstown, NJ). The injection sites were verified and tissue sections from cases with restricted injection sites were further processed for immunohistochemistry.

A sequential set of 30 μm coronal sections through the rostro-caudal extent of the LC and CeA was placed for 30 min in 1% sodium borohydride in 0.1 M PB to remove reactive aldehydes. Sections were then incubated in 0.5% BSA and 0.25% Triton X-100 in 0.1M TBS for 30 min and rinsed extensively in 0.1 M TBS. This was followed by an overnight incubation in a cocktail containing guinea pig antibody directed against prodynorphin (ppDYN; Neuromics, Inc., Minneapolis, MN) at 1:2,000 and CRF antiserum at 1:2,000 (kindly provided by Dr. W. Vale of the Salk Institute) directed against the rat/human form of CRF (Rivier et al., 1983b, Vale et al., 1983). ppDYN and CRF immunoreactivities were visualized using a rhodamine isothiocyanate-conjugated donkey anti-guinea pig (1:200; Jackson Immunoresearch, West Grove, PA) and cyanine dye Cy5-conjugated donkey anti-rabbit (1:200; Jackson Immunoresearch) secondary antibodies, respectively. Control sections were processed in parallel with the tissue sections labeled for ppDYN and CRF with the omission of the respective primary antibodies.

Control and data analysis

For anterograde tract-tracing experiments that were combined with electron microscopy, tissue sections were examined from four rats that exhibited the most restricted placement of anterograde tracer in the CeA and that demonstrated optimal immunocytochemical labeling and preservation of ultrastructural morphology. Control sections were run in parallel where one of the primary antisera was omitted but the rest of the processing procedure was identical. The LC was sampled for electron microscopic analysis. For quantification of labeled profiles in 40 μm-thick sections immunolabeled before embedding for electron microscopy, we have observed that the collection of sections only from the surface of the section minimizes artifacts that may be associated with incomplete penetration of antisera. Tissue sections were collected near the tissue plastic interface but did not exceed a distance of 4 μm from the surface. Digital images of axon terminals containing immunoperoxidase labeling for BDA where dual immunogold-silver labeling for DYN and TH was also present in the neuropil in the fields of at least 11,000X were obtained and later classified. DYN was labeled with large immunogold silver particles measuring at least 0.071 μm in diameter while TH was labeled with small immunogold-silver particles measuring less than 0.071 μm in diameter. At least 10 grids containing 5–8 ultrathin sections were collected from individual Vibratome sections. At least three Vibratome sections were examined per animal. A total sample of 250 BDA-labeled axon terminals was included in the analysis.

The classification of the identified cellular elements were based on the description of Peters and colleagues (Peters and Palay, 1996). Neuronal perikarya were distinguished from proximal dendrites by the presence of a nucleus, Golgi apparatus and smooth endoplasmic reticulum. Dendrites usually contained endoplasmic reticulum and were postsynaptic to axon terminals. Dendrites were defined as proximal if their size was larger than 0.7 μm in diameter. An axon terminal was considered to form a synapse if it showed a junctional complex, a restricted zone of parallel membranes with a slight enlargement of the intercellular space, and/or associated postsynaptic thickening. Asymmetric synapses were identified by thick postsynaptic densities (Gray's type I; (Gray et al., 1984); in contrast, symmetric synapses had thin densities (Gray's type II; (Gray et al., 1984) both pre- and postsynaptically. A non-synaptic contact or apposition was defined as an axon terminal plasma membrane juxtaposed to that of a dendrite or soma devoid of recognizable membrane specializations and no intervening glial processes.

For the retrograde tract-tracing experiment, the percentage of DYN- and CRF-immunoreactive neurons that were retrogradely labeled from the LC was obtained from three rats where fluorescent latex microspheres were utilized as the retrograde tracer. Only animals with discrete injection sites were utilized for data analysis. The criteria for defining a restricted injection sites included an examination of the extent of encroachment on neighboring nuclei. For examination of injection sites, bright field and immunofluorescence images of injection sites (Olympus BX51, Tokyo, Japan) were obtained. Images were then captured using Spot Advanced software (Diagnostic Instruments Inc., Sterling Heights, MI). The percentage of DYN- and CRF-immunoreactive neurons that were retrogradely labeled from the LC were counted in each section (120 μm intervals) according to their rostro-caudal distribution. Cell counts were taken and were represented as mean ± SEM of the numbers of cells found per animal across each series of injections.

Results

Anterograde transport from the CeA to the LC

Figure 1A and C show a representative BDA injection site into the central amygdaloid complex. The placement was targeted primarily to the CeA. Typical injection sites included

sites laterally bounded by the basolateral amygdaloid nucleus and medially by the internal capsule. As we have previously demonstrated (Van Bockstaele et al., 1998), injections of BDA at this level of the CeA showed prominent anterograde transport to the LC. Anterograde transport was prominently detected in fibers and processes distributed within the core of the LC as well as within the pericoerulear area, ventral to the superior cerebellar peduncle, as extensively described in our prior published work (Van Bockstaele et al., 1996a, Van Bockstaele et al., 1998). The anterogradely labeled fibers and processes were thin and varicose and extended into the area medial and slightly dorsal to the mesencephalic nucleus of the trigeminal nerve. Using light microscopy, there was no evidence of retrograde transport in the LC region.

The LC area sampled for ultrastructural analysis included the core of the LC as well as the immediately adjacent pericoerulear area. The pericoerulear area consisted of the region ventromedial to the superior cerebellar peduncle as well as the area dorsomedial to the mesencephalic nucleus of the trigeminal nerve. By electron microscopy, BDA anterogradely labeled axon terminals appeared as an electron dense homogenous reaction product identified in unmyelinated axon terminals (Figure 1D–G, 2). Consistent with the light microscopic data, there was no peroxidase labeling identified in dendrite or perikaryon examined at the ultrastructural level indicating that retrograde transport of BDA did not occur. In BDA-labeled axon terminals that showed dense peroxidase labeling, the distinctive synaptic vesicles were occasionally obscured by the dense peroxidase precipitate (Figure 1F, 2C, 2F). However, BDA-labeled axon terminals that were less densely labeled contained recognizable small, clear vesicles and one or more mitochondria (Figure 1D–E, 2A–B, 2D–E). Some BDA-labeled axon terminals containing DYN targeted non-TH labeled dendrites (Figure 1D, 2C–D). In other cases, BDA-labeled axon terminals and BDA/DYN-labeled axon terminals converged onto common dendrites (Figure 1F).

Monosynaptic projections from amygdalar DYN to LC

Anterograde labeling was combined with sequential dual immunogold-silver labeling where the immunogold-silver particles were differentiated based on their size (Figure 1D, 2). Obtaining different sized immunogold-silver particles was achieved by incubating with one ultrasmall gold conjugate, followed by silver enhancement, and then incubating with the second ultrasmall gold conjugate, followed by additional silver enhancement (Yi et al., 2001). This resulted in two groups of silver-enhanced particles: smaller particles that were enhanced once and larger particles that were enhanced twice (Jin et al., , Yi et al., 2001) Immunoperoxidase- and dual immunogold-silver labeling (large and small gold-silver particles, for DYN and TH, respectively) were localized in the same tissue section (Figure 1D, 2). Gold-silver labeling for DYN and TH were readily distinguishable from each other and were localized to the appropriate cellular structures. DYN was identified by large-sized gold-silver particles (>0.071 μm cross-sectional diameter) while TH was labeled using small-sized gold-silver particles (<0.071 μm cross-sectional diameter). DYN-immunogold-silver particles appeared as black punctate particles within the axon terminals while TH-immunogold-silver particles appeared as smaller black punctate particles within the dendrites and, in very few cases, in axon terminals. Immunogold-silver labeling for DYN and TH was also clearly distinguishable from the immunoperoxidase reaction product. BDA-labeled axon terminals that were less densely labeled and exhibiting DYN immunoreactivity clearly showed abundant heterogeneous vesicles and one to two mitochondria (Figure 1D–E, 2A–B, 2D–E). As described above, the large immunogold-silver particles were clearly distinguishable from the small immunogold-silver ones based on their differing sizes. Thus, small immunogold-silver particles for TH were identified within somatodendritic processes and dendrites, and were occasionally identified in axon terminals. The BDA and DYN were frequently co-localized in axon terminals (Figure 1D–G).

Of 220 BDA-labeled axon terminals where DYN immunoreactivity was present in the neuropil, 74% (162/220) contained DYN immunoreactivity while 26% (58/220) did not contain DYN immunoreactivity. Of the 162 BDA-labeled axon terminals that contained DYN immunoreactivity, 48% (77/162) formed direct contacts with TH-labeled dendrites (Figure 2A–C, E–F) while 52% (85/162) contacted dendrites that could not be unequivocally established as exhibiting TH immunoreactivity (Figure 1G). Of the 77 axon terminals targeting TH-labeled dendrites, 62% (48/77) formed asymmetric-type synapses with TH-labeled dendrites (Figure 2F) while 34% (26/77) formed symmetric-type synapses with TH-labeled dendrites (Figure 2A–B, E). The remaining 4% (3/77) did not show recognizable synaptic specialization with TH-labeled dendrites. Some BDA and DYN-dual labeled axon terminals were apposed to other axon terminals (Figure 2D) but a clear synaptic specialization was not typically present.

LC-projecting amygdalar neurons co-express CRF and DYN

We have previously reported that DYN-immunoreactive fibers are distributed within the core and peri-coerulear subregions of the LC (Reyes et al., 2007b, Reyes et al., 2008). Likewise, independent anatomical evidence has shown that CRF-immunoreactive fibers innervate the LC (Valentino et al., 1992, Van Bockstaele et al., 1996b). Recently, we have demonstrated that DYN- and CRF co-exist in axon terminals in the LC (Reyes et al., 2008). However, the origin of these dually labeled DYN- and CRF-containing axon terminals was not defined. To determine the source of these dually labeled axon terminals, the retrograde tract-tracer, fluorescent latex microspheres was injected into the LC in rats. Of eight experimental subjects receiving an injection into the LC, only three exhibited restricted injection sites and yielded optimal retrograde labeling in the CeA. These were used for the analysis. A representative image of an injection site into the LC is shown in Figure 3A. Injections targeted the region of LC at the level bounded medially by the wall of the fourth ventricle, laterally by the mesencephalic trigeminal tract, ventrally by Barrington's nucleus and dorsally by the superior cerebellar peduncle. In one case, the injection in the LC was centered in the core of the LC (Figure 3A) with little involvement of the pericoerulear area. In two cases, the injections targeted both the LC and included the pericoerulear area adjacent to the superior cerebellar peduncle and included the dorsal part of the core of the LC. This injection was equally effective in producing retrograde labeling in the CeA (Figure 3B). Irrespective of whether green or red fluorescent latex microspheres were employed, there was no appreciable difference in the observed distribution of the retrogradely labeled neurons in the CeA.

Retrogradely labeled neurons were abundant within the CeA. Consistent with our previous reports (Van Bockstaele et al., 1998, Tjoumakaris et al., 2003, Reyes et al., 2008, Rudoy et al., 2009) and those of others (Khachaturian et al., 1982, Swanson et al., 1983, Watson et al., 1983, Fallon and Leslie, 1986, Sakanaka et al., 1986), the CeA is enriched with DYN- as well as CRF-containing perikarya. Moreover, consistent with our recent report (Reyes et al., 2008), a higher number of DYN-immunoreactive neurons were observed compared to CRF (78.33 ± 5.45 vs 60 ± 5.86) in the CeA. Triple labeling immunofluorescence showed retrogradely- (green; Figure 4A,E), DYN- (red; Figure 4B,F) and CRF- (blue; Figure 4C,G) labeled neurons distributed in the CeA. Of the 73 (73.33 ± 5.81) retrogradely labeled neurons, 32% (23/73) contained both DYN and CRF. Approximately 30% (23/78) of CeA neurons projecting to the LC exhibited DYN immunoreactivity while 38% (23/60) exhibited CRF immunoreactivity.

Discussion

Anterograde tract-tracing combined with electron microscopy revealed monosynaptic projections from amygdalar DYN neurons to noradrenergic neurons of the LC. Retrograde

tract-tracing combined with immunofluorescence demonstrated that DYN- and CRF are co-transmitters in CeA-projecting neurons to the LC. Taken together, these multiple lines of evidence establish the importance of peptidergic limbic circuitry in the regulation of LC neurons that may be relevant to stress-related responses.

Methodological considerations

Anterograde and retrograde tract-tracing studies poses certain technical caveats that must be taken into consideration when interpreting results. For example, a limitation of anterograde tract-tracing is the existence of putative retrograde labeling from axonal transport of the tract tracer (Wouterlood and Jorritsma-Byham, 1993). The appearance of retrograde transport of BDA to LC may present a confound for the analysis if the tracer is present in LC neurons with axonal collaterals within the LC. However, consistent with our previous anatomical studies, retrograde transport in LC neurons following BDA injections to the CeA was not observed using light microscopy or at the ultrastructural level. In the present study, BDA injections were primarily restricted to the CeA (Figure 1A–C) and did not extend within neighboring anatomical structures. In addition, the anterograde labeling within the dorsal pontine tegmentum was comparable to the anatomical distribution observed in our previous reports (Van Bockstaele et al., 1996a, Van Bockstaele et al., 1998).

Similar to anterograde transport, technical limitations also exist in retrograde tract-tracing studies including spread of tracer at the injection site as well as uptake and transport from fibers of passage in brain areas adjacent to the injection site. Nevertheless, in the present study retrograde labeling in the CeA is not likely due to significant uptake of tracer from neighboring areas considering that the injection site in the LC did not significantly spread into adjacent brain regions (Figure 3A). Moreover, previous anterograde and retrograde tract-tracing studies support projections from the CeA to the LC (Cedarbaum and Aghajanian, 1978, Wallace et al., 1992, Luppi et al., 1995, Van Bockstaele et al., 1996a, Van Bockstaele et al., 1998). Green and red fluorescent latex microspheres were injected into the LC. Switching between green or red fluorescent latex microspheres did not yield any appreciable difference in retrograde transport to the CeA from the LC.

While acrolein fixation optimizes the preservation of ultrastructural morphology, it produces only limited penetration of immunoreagents in thick tissue sections (Leranth and Pickel, 1989, Chan et al., 1990). As limited penetration of reagents may result in underestimation of the relative frequencies of their distribution, we minimized this caveat by collecting tissue sections near the tissue-Epon interface where penetration is optimal and sampling profiles only when all the markers were present in the surrounding neuropil.

The application of two ultrasmall gold conjugates for the co-localization of two antigens combined with detection of a tract-tracer enabled resolving whether multiple antigens are present in a monosynaptic pathway. Homogeneity of silver enhancement is crucial for creating evenly sized gold-silver particles. However, with any enhancement reagent, some variability is expected (Burry et al., 1992, Rufner et al., 1995, Yi et al., 2001). Considering this variability, we sought a greater difference in the size of gold-silver particles in our ultrastructural analysis. It is likely, though, that our analysis may have under-estimated the number of contacts onto TH-labeled dendrites as we favored shorter silver times for the second sequential enhancement to allow for distinguishing different sized gold particles.

Since it is difficult to detect neuropeptides in soma and dendrites without the use of colchicine, a microtubule inhibitor, we administered this agent intracerebroventricularly twenty hours before euthanasia as described in our previous studies (Reyes et al., 2008). It should be noted, however, that colchicine may induce stress-like responses (Kelly and Watts, 1998) and has been shown to increase mRNA expression levels for certain

neuropeptides (Swanson et al., 1983; Moga et al., 1990). The goal of the present study was to define the phenotype of amygdalar neurons rather than quantify expression levels of peptides. Therefore, although this caveat is noted, it does not impact the interpretation of our results.

Monosynaptic dynorphin projections from amygdala to LC

Using high-resolution ultrastructural analysis, we previously reported that DYN afferents directly target noradrenergic neurons in the LC (Reyes et al., 2007b) and that these form primarily asymmetric (excitatory) type synapses. When combined with immunogold-silver labeling for CRF, single axon terminals were found to contain both peptides (Kreibich et al., 2008). Interestingly, the endogenous opioids DYN and ENK more frequently converge on common postsynaptic targets rather than being co-localized, a finding that is similar to the synaptic organization of CRF and ENK afferents in the LC (Tjoumakaris et al., 2003, Reyes et al., 2007b, Reyes et al., 2008). In the present study, dual-labeled DYN and CRF-axon terminals primarily formed asymmetric (excitatory-type) synapses as compared to symmetric (inhibitory-type) synapses. Asymmetric synapses are thought to be involved principally in excitatory neurotransmission while symmetric synapses are thought to be involved in inhibitory neurotransmission (Peters et al., 1991, Peters and Palay, 1996). There is evidence to support the presence of glutamate in DYN afferents. Vesicular glutamate transporter-1 (VGlut) has been localized within DYN-labeled axon terminals in the LC and these formed primarily asymmetric-type synapses (Barr and Van Bockstaele, 2005). We also reported co-localization of κOR and VGlut in the LC suggesting an interaction between DYN and glutamatergic systems in the amygdalar-LC circuit (Kreibich et al., 2008). It is tempting to speculate that CRF/DYN neurons may be excitatory based on our previous independent studies (Reyes et al., 2008; Reyes et al., 2009) showing CRF and DYN in axon terminals in the LC forming excitatory type synapses. However, considering the large population of gamma-aminobutyric acid (GABA) ergic neurons (Swanson and Petrovich, 1998; Ciocchi et al., 2010) in the amygdala, future studies are required to unequivocally establish whether CRF/DYN neurons in the amygdala are excitatory or inhibitory in nature.

Dynorphin and corticotropin-releasing factor neurons in the CeA project to LC

Using tract-tracing and ultrastructural analysis in independent studies, we have shown that DYN and CRF axon terminals form synaptic specializations with TH-immunoreactive dendrites in the LC (Van Bockstaele et al., 1996b, Reyes et al., 2007b, Reyes et al., 2008). Likewise, using immunofluorescence and electron microscopy, prominent co-existence of DYN and CRF has been demonstrated in varicose processes and axon terminals in the LC region not only in the core but in the pericoerulear region as well (Reyes et al., 2008). Potential sources of DYN and CRF afferent inputs to the LC include the bed nucleus of stria terminalis, CeA, the nucleus of the solitary tract, and the hypothalamus, including the paraventricular nucleus of the hypothalamus (Van Bockstaele et al., 1998, Van Bockstaele et al., 1999a, Van Bockstaele et al., 1999b, Reyes et al., 2005) as they are enriched with DYN- and CRF-containing perikarya (Khachaturian et al., 1982, Watson et al., 1982, Swanson et al., 1983, Watson et al., 1983, Fallon and Leslie, 1986). Dual fluorescence in situ hybridization labeling showed that DYN and CRF are distributed within the CeA where 31% of DYN neurons are co-localized with CRF and 53% of CRF neurons are co-localized with DYN (Reyes et al., 2008). In addition, we and others (Sakanaka et al., 1986) have reported that electrolytic lesions of the CeA significantly decrease CRF immunoreactivity in the LC (Tjoumakaris et al., 2003, Reyes et al., 2008). Similarly, we have shown that electrolytic lesions of the CeA substantially decrease DYN immunoreactivity in the LC (Reyes et al., 2008). Taken together, these independent studies suggested that CRF and DYN innervation of the LC is derived from common limbic sources and we conducted this study to test the hypothesis that CRF and DYN afferents to the LC are derived from

common limbic sources. By combining retrograde and anterograde tract-tracing studies with immunofluorescence and electron microscopy, we provide unequivocal evidence that DYN and CRF afferents to the LC originate, in part, from amygdalar sources (Van Bockstaele et al., 1996b, Van Bockstaele et al., 1998, Reyes et al., 2007b, Reyes et al., 2008).

We were not able to identify whether postsynaptic targets of amygdalar DYN/CRF afferents in the LC are noradrenergic due to the limitation of identifying 4 distinct electron dense markers in the same section of tissue. Combining immunocytochemical detection of three antigens DYN, CRF, TH with a tract tracer (BDA) remains a challenge that has yet to be overcome. However, considering our previous convergent findings of the morphological characteristics of synapses exhibited by singly labeled DYN axon terminals (Reyes et al., 2007b) and dually labeled DYN and CRF axon terminals (Reyes et al., 2008), it is tempting to speculate that axon terminals exhibiting both DYN and CRF immunoreactivities target noradrenergic LC neurons.

Functional implications

The present results suggest an interaction between limbic CRF and DYN circuitry that may play a significant role in the modulation of stress responses in the LC. The DYN/κ-OR system has been implicated in the mediation of stress and vulnerability to drug abuse. For example, stress, which promotes relapse and can facilitate place preference for drugs of abuse, increases prodynorphin gene expression in the limbic system (Shirayama et al., 2004). Genetic deletion of prodynorphin or pharmacological antagonism of kappa receptors prevented stress-induced preference, implicating the DYN/κ-OR system in stress-induced facilitation of drug abuse (Shirayama et al., 2004). Additionally, κ-OR antagonists prevent stress-elicited behaviors that are endpoints of depression such as immobility in the forced swim test and passive behavior in learned helplessness (Mague et al., 2003, McLaughlin et al., 2003, Shirayama et al., 2004). The present findings implicate the LC as one site at which DYN/CRF co-transmission modulates stress responses and the consequences of stress on behavior. Furthermore, the prominent localization of κ-ORs in axon terminals in the LC that contain CRF or the vesicular glutamate transporter, indicate that κ-ORs are poised to presynaptically inhibit diverse afferent signaling to the LC. This is a novel and potentially powerful means of regulating the LC-NE system that can impact on forebrain processing of stimuli and the organization of behavioral strategies in response to environmental stimuli.

The results of this study provide the first ultrastructural evidence that DYN present in axon terminals in the LC arises from the CeA and innervates the noradrenergic LC neurons. Known to play an important role in adaptive responses to stress, the LC is activated by diverse stimuli and is highly responsive to stress (Foote et al., 1983, Aston-Jones et al., 1991). An increase or decrease in the rate and firing pattern of LC neurons determines subsequent behavioral adaptive strategies (Aston-Jones and Cohen, 2005).

Systemic administration of kappa opioiod has anti-depressant- and anxiolytic-like effects (Mague et al., 2003, Shirayama et al., 2004, Knoll et al., 2007). For example, κOR antagonists increased arm exploration in the elevated plus maze and decreased conditioned fear in fear-potentiated startle paradigm (Knoll et al., 2007). These suggest that κOR antagonists may be effective for the treatment of comorbid depressive and anxiety disorders. Intracoerulear microinfusion of the κOR agonist, U50488, did not alter spontaneous discharge but significantly attenuated phasic discharge evoked by sciatic nerve stimulation and auditory, stimuli known to engage excitatory amino acid afferents to the LC (Kreibich et al., 2008). Furthermore, U50488 significantly attenuated tonic LC activation by hypotensive stress, an effect known to be mediated by CRF afferents (Curtis et al., 2002). Thus, results of the present study extend our knowledge of afferent regulation of LC noradrenergic neurons

by demonstrating that opioids and stress peptide, CRF, are co-transmitters in this brain region.

Acknowledgments

This project was supported by National Institutes of Health DA 09082 to E.J.V.B.

References

Arvidsson U, Riedl M, Chakrabarti S, Vulchanova L, Lee JH, Nakano AH, Lin X, Loh HH, Law PY, Wessendorf MW, Elde R. The kappa-opioid receptor is primarily postsynaptic: combined immunohistochemical localization of the receptor and endogenous opioids. Proc Natl Acad Sci U S A. 1995; 92:5062–5066. [PubMed: 7539141]

Aston-Jones G, Cohen JD. An integrative theory of locus coeruleus-norepinephrine function: adaptive gain and optimal performance. Annu Rev Neurosci. 2005; 28:403–450. [PubMed: 16022602]

Aston-Jones, G.; Foote, SL.; Bloom, FE. Anatomy and physiology of locus coeruleus neurons: functional implications. In: Ziegler, M.; Lake, CR., editors. Norepinephrine (Frontiers of Clinical Neuroscience). Williams and Wilkins; Baltimore: 1984. p. 92-116.

Aston-Jones G, Shipley MT, Chouvet G, Ennis M, Van Bockstaele E, Pieribone V, Shiekhattar R, Akaoka H, Drolet G, Astier B. Afferent regulation of locus coeruleus neurons: anatomy, physiology and pharmacology. Prog Brain Res. 1991; 88:47–75. [PubMed: 1687622]

Barr J, Van Bockstaele EJ. Vesicular glutamate transporter-1 colocalizes with endogenous opioid peptides in axon terminals of the rat locus coeruleus. Anat Rec A Discov Mol Cell Evol Biol. 2005; 284:466–474. [PubMed: 15803474]

Burry RW, Vandre DD, Hayes DM. Silver enhancement of gold antibody probes in pre-embedding electron microscopic immunocytochemistry. J Histochem Cytochem. 1992; 40:1849–1856. [PubMed: 1453003]

Cedarbaum JM, Aghajanian GK. Afferent projections to the rat locus coeruleus as determined by a retrograde tracing technique. J Comp Neurol. 1978; 178:1–16. [PubMed: 632368]

Chan J, Aoki C, Pickel VM. Optimization of differential immunogold-silver and peroxidase labeling with maintenance of ultrastructure in brain sections before plastic embedding. J Neurosci Methods. 1990; 33:113–127. [PubMed: 1977960]

Ciocchi S, Herry C, Grenier F, Wolff SB, Letzkus JJ, Vlachos I, Ehrlich I, Sprengel R, Deisseroth K, Stadler MB, Muller C, Luthi A. Encoding of conditioned fear in central amygdala inhibitory circuits. Nature. 2010; 468:277–282. [PubMed: 21068837]

Curtis AL, Bello NT, Connolly KR, Valentino RJ. Corticotropin-releasing factor neurones of the central nucleus of the amygdala mediate locus coeruleus activation by cardiovascular stress. J Neuroendocrinol. 2002; 14:667–682. [PubMed: 12153469]

Curtis AL, Bello NT, Valentino RJ. Evidence for functional release of endogenous opioids in the locus coeruleus during stress termination. J Neurosci. 2001; 21:1–5.

Elde, R.; Hokfelt, T. Coexistence of opioid peptides with other neurotransmitters. In: Herz, A., editor. Handbook of Experimental Pharmacology, Opioids I. Springer; Berlin: 1993. p. 585-624.

Fallon JH, Leslie FM. Distribution of dynorphin and enkephalin peptides in the rat brain. J Comp Neurol. 1986; 249:293–336. [PubMed: 2874159]

Foote SL, Bloom FE, Aston-Jones G. Nucleus locus ceruleus: new evidence of anatomical and physiological specificity. Physiol Rev. 1983; 63:844–914. [PubMed: 6308694]

Gray TS, Cassell MD, Kiss JZ. Distribution of pro-opiomelanocortin-derived peptides and enkephalins in the rat central nucleus of the amygdala. Brain Res. 1984; 306:354–358. [PubMed: 6087978]

Houshyar H, Gomez F, Manalo S, Bhargava A, Dallman MF. Intermittent morphine administration induces dependence and is a chronic stressor in rats. Neuropsychopharmacology. 2003; 28:1960–1972. [PubMed: 12915862]

Jin J, Kittanakom S, Wong V, Reyes BAS, Van Bockstaele EJ, Stagljar I, Berrettini W, Levenson R. Interaction of the mu-opioid receptor with GPR177 (Wntless) inhibits Wnt secretion: potential implications for opioid dependence. BMC Neurosci. 11:33. [PubMed: 20214800]

Kelly AB, Watts AG. The region of the pontine parabrachial nucleus is a major target of dehydration-sensitive CRH neurons in the rat lateral hypothalamic area. J Comp Neurol. 1998; 394:48–63. [PubMed: 9550142]

Khachaturian H, Watson SJ, Lewis ME, Coy D, Goldstein A, Akil H. Dynorphin immunocytochemistry in the rat central nervous system. Peptides. 1982; 3:941–954. [PubMed: 6132365]

Knoll AT, Meloni EG, Thomas JB, Carroll FI, Carlezon WA Jr. Anxiolytic-like effects of kappa-opioid receptor antagonists in models of unlearned and learned fear in rats. J Pharmacol Exp Ther. 2007; 323:838–845. [PubMed: 17823306]

Kreibich AS, Reyes BAS, Curtis AL, Ecke L, Chavkin C, Van Bockstaele EJ, Valentino RJ. Presynaptic inhibition of diverse afferents to the locus coeruleus by kappa opiate receptors: a novel mechanism for regulating the central norepinephrine system. J Neurosci. 2008; 28:6516–6525. [PubMed: 18562623]

Leranth, C.; Pickel, VM. Electron microscopic preembedding double-labeling methods. In: Heimer, L.; Zaborszky, L., editors. Neuroanatomical tracing methods 2. 1. Plenum Press; New York: 1989. p. 129-172.

Luppi PH, Aston-Jones G, Akaoka H, Chouvet G, Jouvet M. Afferent projections to the rat locus coeruleus demonstrated by retrograde and anterograde tracing with cholera-toxin B subunit and Phaseolus vulgaris leucoagglutinin. Neuroscience. 1995; 65:119–160. [PubMed: 7753394]

Mague SD, Pliakas AM, Todtenkopf MS, Tomasiewicz HC, Zhang Y, Stevens WC Jr, Jones RM, Portoghese PS, Carlezon WA Jr. Antidepressant-like effects of kappa-opioid receptor antagonists in the forced swim test in rats. J Pharmacol Exp Ther. 2003; 305:323–330. [PubMed: 12649385]

Maj M, Turchan J, Smialowska M, Przewlocka B. Morphine and cocaine influence on CRF biosynthesis in the rat central nucleus of amygdala. Neuropeptides. 2003; 37:105–110. [PubMed: 12747942]

McLaughlin JP, Marton-Popovici M, Chavkin C. Kappa opioid receptor antagonism and prodynorphin gene disruption block stress-induced behavioral responses. J Neurosci. 2003; 23:5674–5683. [PubMed: 12843270]

McNally GP, Akil H. Role of corticotropin-releasing hormone in the amygdala and bed nucleus of the stria terminalis in the behavioral, pain modulatory, and endocrine consequences of opiate withdrawal. Neuroscience. 2002; 112:605–617. [PubMed: 12074902]

Moga MM, Saper CB, Gray TS. Neuropeptide organization of the hypothalamic projection to the parabrachial nucleus in the rat. J Comp Neurol. 1990; 295:662–682. [PubMed: 1972710]

Paxinos, G.; Watson, C. The rat brain in stereotaxic coordinates. Academic Press; New York: 1986.

Peters A, Palay SL. The morphology of synapses. J Neurocytol. 1996; 25:687–700. [PubMed: 9023718]

Peters, A.; Palay, SL.; Webster, Hd. The Fine Structure of the Nervous System. Oxford University Press; New York: 1991.

Reyes BAS, Chavkin C, van Bockstaele EJ. Subcellular targeting of kappa-opioid receptors in the rat nucleus locus coeruleus. J Comp Neurol. 2009; 512:419–431. [PubMed: 19009591]

Reyes BAS, Drolet G, Van Bockstaele EJ. Dynorphin and stress-related peptides in rat locus coeruleus: contribution of amygdalar efferents. J Comp Neurol. 2008; 508:663–675. [PubMed: 18381633]

Reyes BAS, Glaser JD, Van Bockstaele EJ. Ultrastructural evidence for co-localization of corticotropin-releasing factor receptor and mu-opioid receptor in the rat nucleus locus coeruleus. Neurosci Lett. 2007; 413:216–221. [PubMed: 17194545]

Reyes BAS, Valentino RJ, Xu G, Van Bockstaele EJ. Hypothalamic projections to locus coeruleus neurons in rat brain. Eur J Neurosci. 2005; 22:93–106. [PubMed: 16029199]

Reyes BAS, Johnson AD, Glaser JD, Commons KG, Van Bockstaele EJ. Dynorphin-containing axons directly innervate noradrenergic neurons in the rat nucleus locus coeruleus. Neuroscience. 2007; 145:1077–1086. [PubMed: 17289275]

Rivier J, Spiess J, Vale W. Characterization of rat hypothalamic corticotropin-releasing factor. Proceedings of the National Academy of Sciences of the United States of America. 1983; 80:4851–4855. [PubMed: 6603620]

Rudoy CA, Reyes AR, Van Bockstaele EJ. Evidence for beta1-adrenergic receptor involvement in amygdalar corticotropin-releasing factor gene expression: implications for cocaine withdrawal. Neuropsychopharmacology. 2009; 34:1135–1148. [PubMed: 18596687]

Rufner R, Carson NE, Forte M, Danscher G, Gu J, Hacker GW. Autometallography for imunogold–silver staining in light and electron microscopy. Cell Vis. 1995; 2:327–333.

Sakanaka M, Shibasaki T, Lederis K. Distribution and efferent projections of corticotropin-releasing factor-like immunoreactivity in the rat amygdaloid complex. Brain Res. 1986; 382:213–238. [PubMed: 2428439]

Sawchenko PE, Swanson LW, Vale WW. Co-expression of corticotropin-releasing factor and vasopressin immunoreactivity in parvocellular neurosecretory neurons of the adrenalectomized rat. Proc Natl Acad Sci U S A. 1984; 81:1883–1887. [PubMed: 6369332]

Shirayama Y, Ishida H, Iwata M, Hazama GI, Kawahara R, Duman RS. Stress increases dynorphin immunoreactivity in limbic brain regions and dynorphin antagonism produces antidepressant-like effects. J Neurochem. 2004; 90:1258–1268. [PubMed: 15312181]

Swanson LW, Petrovich GD. What is the amygdala? Trends Neurosci. 1998; 21:323–331. [PubMed: 9720596]

Swanson LW, Sawchenko PE, Rivier J, Vale WW. Organization of ovine corticotropin-releasing factor immunoreactive cells and fibers in the rat brain: an immunohistochemical study. Neuroendocrinology. 1983; 36:165–186. [PubMed: 6601247]

Tjoumakaris SI, Rudoy C, Peoples J, Valentino RJ, Van Bockstaele EJ. Cellular interactions between axon terminals containing endogenous opioid peptides or corticotropin-releasing factor in the rat locus coeruleus and surrounding dorsal pontine tegmentum. J Comp Neurol. 2003; 466:445–456. [PubMed: 14566941]

Vale WW, Rivier C, Brown MR, Spiess J, Koob G, Swanson L, Bilezikjian L, Bloom F, Rivier J. Chemical and biological characterization of corticotropin releasing factor. Rec Prog Horm Res. 1983; 39:245–270. [PubMed: 6314446]

Valentino RJ, Page M, Van Bockstaele E, Aston-Jones G. Corticotropin-releasing factor innervation of the locus coeruleus region: distribution of fibers and sources of input. Neuroscience. 1992; 48:689–705. [PubMed: 1376457]

Valentino RJ, Page ME, Curtis AL. Activation of noradrenergic locus coeruleus neurons by hemodynamic stress is due to local release of corticotropin-releasing factor. Brain Res. 1991; 555:25–34. [PubMed: 1933327]

Van Bockstaele EJ, Chan J, Pickel VM. Input from central nucleus of the amygdala efferents to pericoerulear dendrites, some of which contain tyrosine hydroxylase immunoreactivity. J Neurosci Res. 1996; 45:289–302. [PubMed: 8841990]

Van Bockstaele EJ, Colago EEO, Valentino RJ. Corticotropin-releasing factor-containing axon terminals synapse onto catecholamine dendrites and may presynaptically modulate other afferents int he rostral pole of the nucleus locus coeruleus in the rat brain. J Comp Neurol. 1996; 364:523–534. [PubMed: 8820881]

Van Bockstaele EJ, Colago EEO, Valentino RJ. Amygdaloid corticotropin-releasing factor targets locus coeruleus dendrites: substrate for the co-ordination of emotional and cognitive limbs of the stress response. J Neuroendocrin. 1998; 10:743–757.

Van Bockstaele EJ, Peoples J, Telegan P. Efferent projections of the nucleus of the solitary tract to peri-locus coeruleus dendrites in rat brain: evidence for a monosynaptic pathway. J Comp Neurol. 1999; 412:410–428. [PubMed: 10441230]

Van Bockstaele EJ, Peoples J, Valentino RJ. A.E. Bennett Research Award. Anatomic basis for differential regulation of the rostrolateral peri-locus coeruleus region by limbic afferents. Biol Psychiatry. 1999; 46:1352–1363. [PubMed: 10578450]

Van Bockstaele EJ, Pickel VM. Ultrastructure of serotonin-immunoreactive terminals in the core and shell of the rat nucleus accumbens: cellular substrates for interactions with catecholamine afferents. J Comp Neurol. 1993; 334:603–617. [PubMed: 8408768]

Wallace DM, Magnuson DJ, Gray TS. Organization of amygdaloid projections to brainstem dopaminergic, noradrenergic, and adrenergic cell groups in the rat. Brain Res Bull. 1992; 28:447–454. [PubMed: 1591601]

Watson SJ, Khachaturian H, Akil H, Coy DH, Goldstein A. Comparison of the distribution of dynorphin systems and enkephalin systems in brain. Science. 1982; 218:1134–1136. [PubMed: 6128790]

Watson SJ, Khachaturian H, Taylor L, Fischli W, Goldstein A, Akil H. Pro-dynorphin peptides are found in the same neurons throughout rat brain: immunocytochemical study. Proc Natl Acad Sci U S A. 1983; 80:891–894. [PubMed: 6131416]

Wouterlood FG, Jorritsma-Byham B. The anterograde neuroanatomical tracer biotinylated dextran-amine: comparison with the tracer Phaseolus vulgaris-leucoagglutinin in preparations for electron microscopy. J Neurosci Methods. 1993; 48:75–87. [PubMed: 7690870]

Yi H, Leunissen J, Shi G, Gutekunst C, Hersch S. A novel procedure for pre-embedding double immunogold-silver labeling at the ultrastructural level. J Histochem Cytochem. 2001; 49:279–284. [PubMed: 11181730]

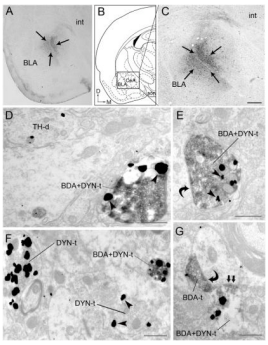

Figure 1.

A. Low magnification brightfield photomicrograph of a representative BDA injection into the CeA in the rat brain. Arrows indicate neurons exhibiting peroxidase labeling for BDA at the injection site. **B.** A schematic diagram adapted from the rat brain atlas of Paxinos and Watson (Paxinos and Watson, 1986) showing the anterior posterior level of the region of the central amygdaloid complex targeted for injection placement. Arrows indicate dorsal (D) and medial (M) orientation. Panel C shows a higher magnification view of panel A and reflects the level shown in the schematic from panel B. **D.** Electron photomicrograph showing immunoperoxidase labeling for biotinylated dextran amine (BDA) and dual immunogold-silver labeling for dynorphin (DYN; large gold) and tyrosine hydroxylase (TH; small gold) in the locus coeruleus. Dense peroxidase labeling can be seen in a BDA-labeled axon terminal containing large gold-silver grains (arrowheads) that indicate labeling for DYN (BDA+DYN-t). In a separate profile, a dendrite containing TH.can be seen by the presence of small gold-silver labeling. **E.** A BDA+DYN-t forms a symmetric synapse (curved arrow) with a dendrite that lacks detectable immunoreactivity for TH. **F.** Two DYN-labeled axon terminals that do not contain BDA can be seen in proximity to a BDA+DYN-t. **G.** A BDA-labeled terminal and a BDA+DYN-t converge on a TH-labeled dendrite. A BDA-labeled terminal forms a symmetric synapse (curved arrow) while BDA+DYN-t forms an asymmetric synapse (arrows) with a dendrite. ud, unlabeled dendrite. CeA, central nucleus of the amygdala; int, internal capsule; son, supraoptic nucleus. Scale bar for panel C = 100 μm. Scale bar for panels D–G = 0.50 μm

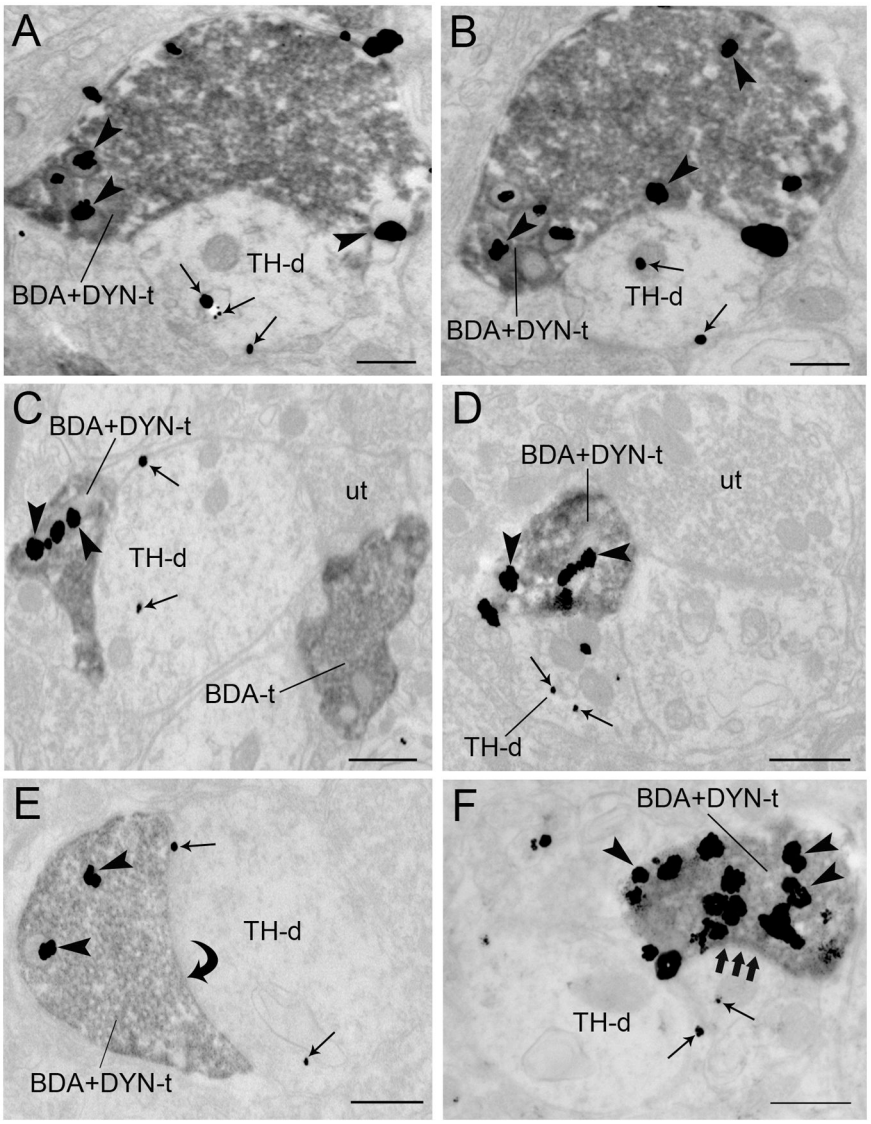

Figure 2.

Electron photomicrograph showing immunoperoxidase labeling for biotinylated dextran amine (BDA) and dual immunogold-silver labeling for dynorphin (DYN) and tyrosine hydroxylase (TH) in the locus coeruleus. **A–B.** Two adjacent sections showing a BDA-labeled axon terminal containing dynorphin (BDA+DYN-t) contacting a TH-labeled dendrite (TH-d). DYN-t is labeled with large gold particles (arrowheads) while TH-t is labeled with small gold particles (arrows). **C.** A BDA+DYN-t and a BDA-labeled axon terminal (BDA-t) converge on a TH-d. The BDA-t is also apposed to an unlabeled terminal (ut) that also contacts the TH-d. **D.** A BDA+DYN-t is seen contacting a TH-d, and is also apposed to an unlabeled axon terminal (ut). **E.** A BDA+DYN-t forms a symmetric synapse (curved arrow) with a TH-d. **F.** A BDA+DYN-t forms an asymmetric synapse (multiple arrows) with a TH-d. Arrows point to small immunogold-silver particles that indicate TH immunoreactivity. Arrowheads point to large immunogold silver particles that denote DYN immunoreactivity. Scale bars = 0.05 μm.

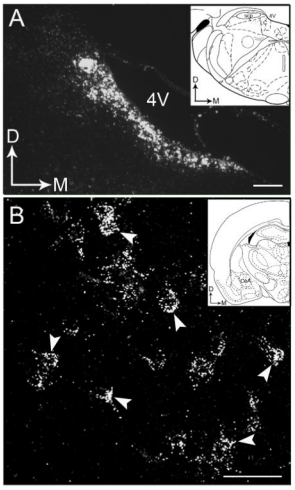

Figure 3.

A. Photomicrograph showing a representative tracer injection of green fluorescent latex microspheres into the LC. **B.** Photomicrograph showing representative retrogradely labeled neurons in the CeA following an injection into the LC. Insets in panels A and B show schematic diagrams adapted from the rat brain atlas of Paxinos and Watson (Paxinos and Watson, 1986) indicating the anterior posterior level of the representative injection site in the LC and retrograde labeling in the CeA. Arrows indicate dorsal (D) and medial (M) orientation of the sections. Arrowheads point to retrogradely labeled neurons in the CeA. CeA, central nucleus of the amygdala; LC, locus coeruleus; 4V, fourth ventricle; scp, superior cerebellar peduncles. Scale bar, 100 μm.

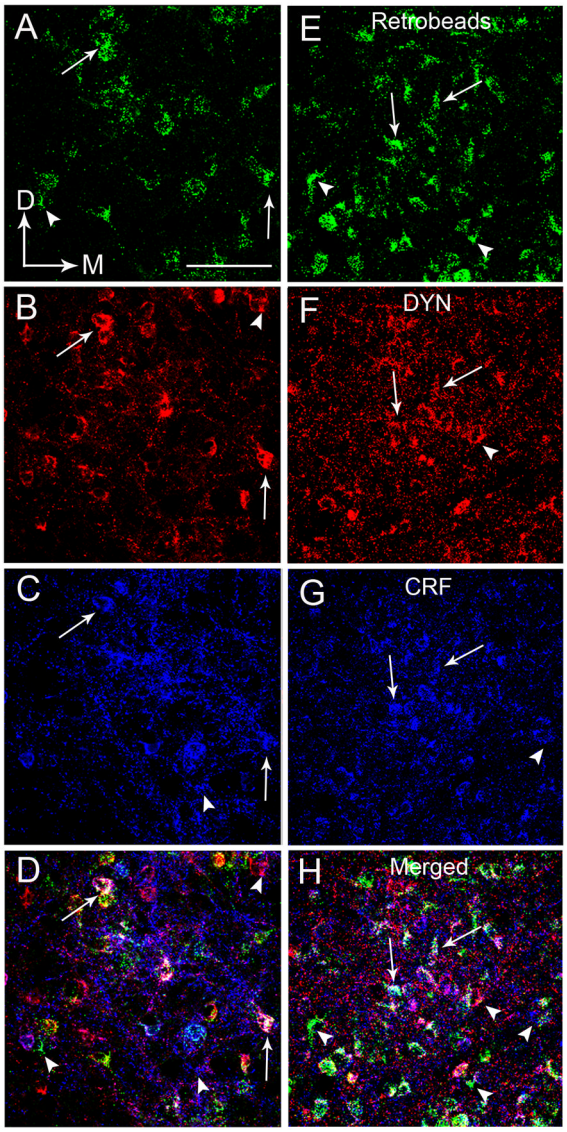

Figure 4.

High magnification photomicrographs illustrating retrograde transport from the LC to the CeA. Retrogradely labeled neurons in the CeA (**A and E**) contain DYN (**B and F**) and CRF (**C and G**). DYN immunolabeling was detected using a rhodamine isothiocyanate-tagged secondary antibody (red; **B and F**). Arrowheads point to individual DYN-immunoreactive neurons that contain only DYN. CRF immunolabeling was detected using a Cy5-tagged secondary antibody (blue; **C and G**). Arrowheads point to individual CRF-immunoreactive neurons that contain only CRF. **D and H** are merged images of A–C and E–G, respectively. Arrows point to single neurons that contain CRF, DYN and retrobeads. Arrowheads denote neurons that exhibit retrobeads, DYN or CRF only. Scale bar, 100 μm.